

## Neutron-spectroscopic strength in Ru isotopes

J. L. M. Duarte, T. Borello-Lewin, and L. B. Horodyski-Matsushigue  
*Instituto de Física da Universidade de São Paulo, São Paulo, Brasil*

(Received 22 February 1994)

A systematic, high resolution (6–8 keV) study of ( $d, t$ ) reactions on  $^{100,102,104}\text{Ru}$  is reported. Spectroscopic factors were extracted by comparison of experimental angular distributions with distorted wave Born approximation predictions. All of the information for  $^{99}\text{Ru}$  and, for excitation energies above 0.9 MeV, for  $^{103}\text{Ru}$  is new. Most of the strength expected for the 50–82 neutron shell was found. The strength distributions are discussed, also in comparison with the corresponding stripping reactions. Special attention is focused on extremely low and relatively intense  $l = 3$  excitations and on the  $l = 4$  transfer pattern observed.

PACS number(s): 25.45.Hi, 27.60.+j, 21.10.Jx

### I. INTRODUCTION

The precise location of single particle and hole spectroscopic strengths is a powerful tool in pinning down nuclear structure properties, since the spreading pattern thus determined is a sensitive test on detailed model predictions [1,2]. In the spherical independent particle shell model the one particle or hole configuration is concentrated at a unique excitation energy. Any collective correlations tend to wash this feature out, in a way which is characteristic of the interactions considered [2,3]. Thus any sudden structure transition should, in particular, also be evidenced through an abrupt change in the particle and hole strength distributions. A survey of the literature reveals, however, that in the challenging region around the  $A = 100$  nuclides [4] the information on these strengths is far from complete [5–7]. The interest in a precise and comparative study of, in particular, the Ru isotopes through transfer reactions was furthermore fostered by the discovery of an intense  $l = 3$  transition at low excitation energy in the  $^{100}\text{Ru}(d, p)^{101}\text{Ru}$  reaction measured by the USP Nuclear Emulsion Group [8]. The present paper refers to results obtained at the São Paulo spectrograph facility for the  $^{100,102,104}\text{Ru}(d, t)^{99,101,103}\text{Ru}$  reactions, which located most of the hole spectroscopic strength in the odd isotopes.

### II. EXPERIMENTAL PROCEDURE

The deuteron beam of the São Paulo Pelletron accelerator, with an incident energy of, respectively, 15.5 and 16.0 MeV, was focused on  $^{100}\text{Ru}$  and  $^{102,104}\text{Ru}$  enriched targets, after passing defining slits of  $1.0 \times 3.0 \text{ mm}^2$ . Table I presents the isotopic compositions of the Ru metal used, in powder form, for target preparation in a well controlled electron bombardment evaporation technique [9,10]. The ejectiles of the reactions were momentum analyzed by the Enge split-pole spectrograph and detected in nuclear emulsion (Kodak NTB or NTA 50  $\mu\text{m}$  thick). The careful determination of the focal plane of the respective reaction, the use of nuclear emulsions, uniform

targets, adequate spectrograph objects, and also good accelerator characteristics, resulted in energy resolutions from 6 to 8 keV, almost determined by the intrinsic resolution of the spectrograph. The emulsion plates were scanned, after processing, in strips of 200  $\mu\text{m}$  across the plates. Typical spectra for the three reactions are presented in Fig. 1.

Relative normalization of the spectra obtained at each angle was achieved by measuring the beam current in an aligned Faraday cup, with electron suppression, connected to a current integrator, while continuously monitoring the direction of the beam. Absolute normalization of the cross sections was referred to optical-model predictions for the elastic scattering of deuterons on the same target, measured under similar conditions. Three well-established families from the systematics of Perey and Perey (PP) [11], Lohr and Haerberli (LH) [12], and Daehnick *et al.* (DCV) [13] (see Table II) were employed and produced cross sections which differed in at most  $\pm 11\%$ . Due, furthermore, to target nonuniformity, plate scanning, and statistics in the elastic scattering data, a maximum uncertainty of 15% is estimated for the absolute cross section scale.

The parameters identified as PP (with the spin orbit term taken from LH) were finally chosen for the absolute normalization of the cross sections and also to generate the distorted incident waves. The distorted wave Born approximation (DWBA) calculations were performed with the code DWUCK4 (Ref. [14]), with usual corrections to account for finite range and nonlocality effects. The outgoing triton channel was described by the optical-model parameters of the systematics by Becchetti

TABLE I. Isotopic composition of the targets.

Target	Composition specified by fabricant (ORNL)						
	$^{96}\text{Ru}$	$^{98}\text{Ru}$	$^{99}\text{Ru}$	$^{100}\text{Ru}$	$^{101}\text{Ru}$	$^{102}\text{Ru}$	$^{104}\text{Ru}$
$^{100}\text{Ru}$	0.05	0.05	0.54	97.24	1.20	0.83	0.19
$^{102}\text{Ru}$	0.02	0.01	0.07	0.09	0.24	99.35	0.22
$^{104}\text{Ru}$	0.02	0.02	0.08	0.13	0.27	3.14	96.39

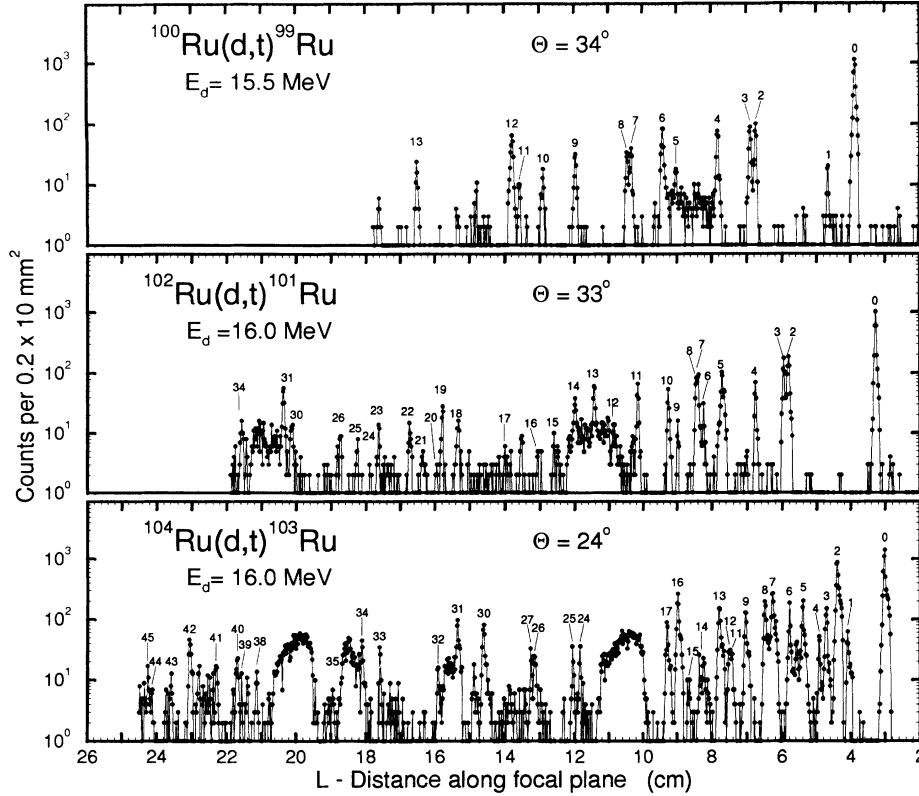


FIG. 1. Spectra of tritons emerging from  $^{100,102,104}\text{Ru}(d,t)$  reactions at the angles indicated.

TABLE II. Optical parameters employed in the DWBA calculations.

Colliding nuclei	Parameter set <sup>a</sup>	$V_R$ (MeV)	$r_R$ (fm)	$a_R$ (fm)	$V_{SO}$ (MeV)	$r_{SO}$ (fm)	$a_{SO}$ (fm)	$W$ (MeV)	$r_W$ (fm)	$a_W$ (fm)	$W_D$ (MeV)	$r_D$ (fm)	$a_D$ (fm)
$^{100}\text{Ru}+d$	PP	96.55	1.15	0.81							18.12	1.34	0.68
	LH	111.98	1.05	0.86	7.00	0.75	0.50				10.12	1.43	0.78
	DCV	92.81	1.17	0.74	6.88	1.07	0.66	1.81	1.33	0.86	10.79	1.33	0.86
$^{102}\text{Ru}+d$	PP	96.31	1.15	0.81							18.24	1.34	0.68
	LH	111.85	1.05	0.86	7.00	0.75	0.50				9.99	1.43	0.78
	DCV	92.63	1.17	0.74	6.87	1.07	0.66	1.87	1.33	0.86	10.75	1.33	0.86
$^{104}\text{Ru}+d$	PP	96.19	1.15	0.81							18.24	1.34	0.68
	LH	111.71	1.05	0.86	7.00	0.75	0.50				9.86	1.43	0.79
	DCV	92.57	1.17	0.74	6.87	1.07	0.66	1.87	1.33	0.86	10.75	1.33	0.86
$^A\text{Ru}+n$	BG	<sup>b</sup>	1.17	0.75			$\lambda_{SO} = 25^c$						
$^{99}\text{Ru}+t$	BG	164.29						33.78					
		$-0.17 E_t$	1.20	0.72	2.50	1.20	0.72	$-0.33 E_t$	1.40	0.88			
$^{101}\text{Ru}+t$	BG	164.18						31.84					
		$-0.17 E_t$	1.20	0.72	2.50	1.20	0.72	$-0.33 E_t$	1.40	0.88			
$^{103}\text{Ru}+t$	BG	164.07						29.98					
		$-0.17 E_t$	1.20	0.72	2.50	1.20	0.72	$-0.33 E_t$	1.40	0.88			

<sup>a</sup>PP: Reference [11].

LH: Reference [12].

DCV: Reference [13].

BG: Reference [15].

<sup>b</sup>Adjusted by well-matching procedure.

<sup>c</sup>Thomas factor.

and Greenlees [15], presented in Table II, where the geometrical parameters of the bound neutron potential are also shown. Except for the  $1g_{9/2}$ ,  $3p$ , and  $2f$  orbits, the neutron single particle orbitals taken were those of the 50–82 shell.

The spectroscopic intensities  $C^2 S_{lj}$  were extracted by comparing measured and calculated angular cross section distributions through the expression

$$C^2 S_{lj} = \frac{1}{3.33} (2j + 1) \frac{\sigma_{\text{exp}}(\theta)}{\sigma_{\text{DW}}(\theta)},$$

where  $\sigma_{\text{DW}}(\theta)$  are the cross sections predicted by the DWBA analysis for the transfer of a neutron with orbital angular momentum  $l$  and total spin  $j$  from the even Ru to the incident deuteron. The factor  $(3.33)^{-1}$  is due to the overlap of the triton and deuteron wave functions, taken, respectively, in the Irving-Gunn and Hulthén descriptions [16].

The differences in  $\sigma_{\text{DW}}(\theta)$  produced by the three deuteron optical-model sets in use are at most  $\pm 15\%$ , while the shapes of the curves are practically not changed.

The excitation energy scale was set by internal calibration through strong transitions clearly identified with levels reported in  $\gamma$ -ray studies and indicated by asterisks in Tables III, IV, and V. The resulting calibration of the spectrograph focal plane was compatible with

the calibration in common use, taken over a greater interval of bending radii, through the analysis of the  $^{90}\text{Zr}(\alpha, \alpha')$  reaction up to 5.9 MeV of excitation. The excitation energies presented in Tables III, IV, and V for the states populated by one neutron transfer were obtained as mean values of the energies calculated at each angle with the aid of a relativistic kinematics code. The tables present excitation energy values whenever a level was clearly isolated at least at three angles, but to be included in Figs. 2–4 an angular distribution had to consist of a minimum of five experimental points.

### III. RESULTS

#### A. The $^{100}\text{Ru}(d, t)^{99}\text{Ru}$ reaction

No previous stripping or pick-up work leading to  $^{99}\text{Ru}$  is reported in the literature. Table III and Fig. 2 present the findings of the present work, for which the excitation energy region accessible to clean study is limited to 1.4 MeV by the appearance, on the focal plane, of the elastic peak and its associated tail. The detection limit below 1.4 MeV is  $\sim 9 \mu\text{b}/\text{sr}$  and above this excitation energy it is  $\sim 150 \mu\text{b}/\text{sr}$ . The level energies shown in Table III are characterized by standard deviations which are typically 1 keV and are never more than 2 keV. Of the 14 levels clearly identified, nine could be associated to

TABLE III. Experimental results for  $^{99}\text{Ru}$  from the  $^{100}\text{Ru}(d, t)$  reaction in comparison with the levels adopted by Nuclear Data Sheets. The asterisk denotes levels used in energy calibration.

Level number	Present Work					Nuclear data <sup>a</sup>	
	$E_{\text{exc}}$ (MeV)	$[\sigma_{\text{exp}}(\theta)]_{\text{max}}$ (mb/sr)	$l$	$j$	$C^2 S_{lj}$	$E_{\text{exc}}$ (MeV)	$J^\pi$
0	0.000*	4.2±0.3	2	5/2	1.8	0.00000	5/2 <sup>+</sup>
1	0.090	0.077±0.013	(2)	(3/2)	(0.037)	0.08968	3/2 <sup>+</sup>
2	0.322*	0.32±0.03	2	5/2; 3/2	0.20; 0.25	0.32237	(3/2) <sup>+</sup>
3	0.340	0.19±0.02	4	7/2	1.8	0.34074	7/2 <sup>+</sup>
4	0.442*	0.84±0.10	0	1/2	0.13	0.44271	(1/2) <sup>+</sup>
5	0.576	0.028±0.009				0.57589	(5/2) <sup>+</sup>
						0.61791	7/2 <sup>+</sup>
6	0.618*	0.76±0.10	0	1/2	0.16	0.61803	(1/2) <sup>+</sup>
7	0.719*	0.083±0.008	4	9/2	0.55	0.71987	9/2 <sup>+</sup>
8	0.734	0.12±0.02				0.73413	(5/2) <sup>+</sup>
9	0.897*	0.115±0.010	2	5/2; 3/2	0.057; 0.069	0.89692	(1/2 <sup>+</sup> ; 3/2; 5/2 <sup>+</sup> )
10	1.000	0.050±0.017				0.99874	(1/2 <sup>+</sup> ; 3/2; 5/2 <sup>+</sup> )
						1.04863	(11/2) <sup>+</sup>
11	1.072	0.034±0.010	(5)	(11/2)	(0.55)	1.06994	11/2 <sup>-</sup>
12	1.093 <sup>b</sup>	0.26±0.03	2	5/2; 3/2	0.24; 0.30		
						1.1184	(7/2 <sup>+</sup> )
						1.2007	
						1.26124	7/2 <sup>+</sup>
						1.27759	(7/2 <sup>+</sup> ; 9/2 <sup>+</sup> )
						1.29078 <sup>c</sup>	7/2 <sup>-</sup>
						1.3061	(7/2 <sup>+</sup> )
						1.3199	(11/2 <sup>+</sup> )
13	1.385	0.13±0.05				1.38316	(1/2 <sup>+</sup> ; 3/2)

<sup>a</sup>Reference [5].

<sup>b</sup>Possible doublet.

<sup>c</sup>Levels observed in Ref. [17].

TABLE IV. Experimental results for  $^{101}\text{Ru}$  from the  $^{102}\text{Ru}(d, t)$  reaction in comparison with previous transfer studies and the levels adopted by Nuclear Data Sheets. The asterisk denotes levels used in energy calibration.

Level number	Present work					$(p, d)^a$					$(d, p)^b$					Nuclear data <sup>c</sup>	
	$E_{\text{exc}}$ (MeV)	$[\sigma_{\text{exp}}(\theta)]_{\text{max}}$ (mb/sr)	$l$	$j$	$C^2S_{ij}$	$E_{\text{exc}}$ (MeV)	$l$	$C^2S_{ij}$	$E_{\text{exc}}$ (MeV)	$l$	$C^2S_{ij}$	$E_{\text{exc}}$ (MeV)	$l$	$C^2S_{ij}$	$E_{\text{exc}}$ (MeV)	$J^\pi$	
0	0.000*	$5.62 \pm 0.23$	2	5/2	1.8	0.000	2	2.25	0.000	2	2.1	0.00000	2	2.1	0.00000	5/2 <sup>+</sup>	
1	0.127	$0.015 \pm 0.004$	(2)	(3/2)	(0.006)	0.127	2	0.013	0.127	2	0.067	0.12723	2	0.067	0.12723	3/2 <sup>+</sup>	
2	0.307		4	7/2	2.3		4	2.86	0.307	4	5.3	0.30685	4	5.3	0.30685	7/2 <sup>+</sup>	
2'	0.311	$0.56 \pm 0.04^d$	2	5/2; 3/2	0.19; 0.23		2	0.29		2		0.31133	2		0.31133	5/2 <sup>+</sup> ; 3/2 <sup>+</sup>	
3	0.324*	$2.43 \pm 0.12$	0	1/2	0.32	0.325 <sup>e</sup>	0	0.16	0.326	0	0.96	0.3248	0	0.96	0.3248	1/2 <sup>+</sup>	
4	0.421*	$0.38 \pm 0.06$	2	3/2	0.22	0.422	2	0.20	0.421	2	0.15	0.4223	2	0.15	0.4223	3/2 <sup>+</sup>	
5	0.534 <sup>f</sup>	$0.57 \pm 0.04^g$	5	11/2	1.2	0.540 <sup>e</sup>	5	0.99		5	5.8	0.5275	5	5.8	0.5275	11/2 <sup>-</sup>	
6	0.597	$0.15 \pm 0.02$	2	5/2; 3/2	0.26; 0.33		2	0.27; 0.34	0.533 <sup>e</sup>	2	0.72; 0.75	0.535	2	0.72; 0.75	0.535	5/2 <sup>+</sup> ; 3/2 <sup>+</sup>	
7	0.615	$0.61 \pm 0.06$	3	7/2; 5/2	0.09; 0.13		3	0.31; 0.40	0.597	3	0.60; 0.74	0.54508	3	0.60; 0.74	0.54508	7/2 <sup>+</sup>	
8	0.622*	$1.07 \pm 0.10$	0	1/2	0.12	0.623 <sup>e</sup>	0	0.063	0.622	0	0.063	0.6235	0	0.063	0.6235	1/2 <sup>+</sup>	
9	0.684	$0.062 \pm 0.007$	(1)	(3/2; 1/2)	(0.007; 0.009)	0.687	2	0.024; 0.031	0.685	2	0.17; 0.18	0.684	2	0.17; 0.18	0.684	5/2 <sup>+</sup> ; 3/2 <sup>+</sup>	
10	0.719	$0.135 \pm 0.015$	4	9/2	0.50	0.720	4	0.29	0.718	1	0.017; 0.018	0.718	1	0.017; 0.018	0.718	3/2 <sup>-</sup> ; 1/2 <sup>-</sup>	
11	0.824	$0.32 \pm 0.03$	2	5/2; 3/2	0.18; 0.22	0.822	2	0.13; 0.17	0.742			0.823	2	0.40; 0.43	0.823	5/2 <sup>+</sup> ; 3/2 <sup>+</sup>	
12	0.907	$0.09 \pm 0.02$	1	3/2; 1/2	0.011; 0.012	0.927	2	0.048; 0.062	0.908	1	0.057; 0.060	0.908	1	0.057; 0.060	0.908	(7/2) <sup>+</sup>	
13	0.974	$0.25 \pm 0.02$	2	5/2; 3/2	0.14; 0.18	0.975	2	0.14; 0.17	0.972	2	0.63; 0.70	0.9734	2	0.63; 0.70	0.9734	3/2 <sup>-</sup> ; 1/2 <sup>-</sup>	
14	1.038	$0.15 \pm 0.02$	2	5/2; 3/2	0.08; 0.10	1.041	2	0.094; 0.12				1.0012			1.0012	5/2 <sup>+</sup> ; 3/2 <sup>+</sup>	
15	1.111	$0.13 \pm 0.02$	0	1/2	0.022	1.112	0	0.012	1.051	4	0.28	1.051	4	0.28	1.051	(7/2) <sup>+</sup>	
16	1.164	$0.054 \pm 0.008$				1.169	2	0.036; 0.045	1.098	0	0.028	1.098	0	0.028	1.098	15/2 <sup>-</sup>	
17	1.266	$0.026 \pm 0.010$				1.225	4	0.19; 0.33	1.112	0	0.17	1.110	0	0.17	1.110	5/2 <sup>+</sup> ; 3/2 <sup>+</sup>	
18	1.425	$0.047 \pm 0.009$				1.276	0	0.011	1.227	0	0.016	1.225	0	0.016	1.225	9/2 <sup>+</sup> ; 7/2 <sup>+</sup>	
						1.268	2	0.019; 0.022	1.276	2	0.019; 0.022	1.268	2	0.019; 0.022	1.268	1/2 <sup>+</sup>	
						1.276	0	0.011	1.276	0	0.011	1.276	0	0.011	1.276	5/2 <sup>+</sup> ; 3/2 <sup>+</sup>	
						1.440			1.3215			1.3215			1.3215	1/2 <sup>+</sup>	
						1.440			1.3899			1.3899			1.3899	(11/2 <sup>+</sup> )	

TABLE IV. (Continued).

Level number	Present work					$(p, d)^a$			$(d, p)^b$			Nuclear data <sup>c</sup>	
	$E_{\text{exc}}$ (MeV)	$[\sigma_{\text{exp}}(\theta)]_{\text{max}}$ (mb/sr)	$l$	$j$	$C^2S_{lj}$	$E_{\text{exc}}$ (MeV)	$l$	$C^2S_{lj}$	$E_{\text{exc}}$ (MeV)	$l$	$C^2S'_{lj}$	$E_{\text{exc}}$ (MeV)	$J^\pi$
19	1.477	$0.19 \pm 0.02$	2	5/2; 3/2	0.11; 0.13	1.510	2	0.16; 0.20	1.501			1.4993	13/2 <sup>+</sup>
20	1.498	$0.014 \pm 0.006$										1.5010	5/2 <sup>+</sup> ; 3/2 <sup>+</sup>
21	1.542	$0.04 \pm 0.02$				1.555	2	0.055; 0.065	1.544			1.510 <sup>i</sup>	5/2 <sup>+</sup> ; 3/2 <sup>+</sup>
22	1.585	$0.082 \pm 0.009$	2	5/2; 3/2	0.063; 0.079	1.597	2	0.085; 0.100	1.584	2	0.45; 0.50	1.555	5/2 <sup>+</sup> ; 3/2 <sup>+</sup>
												1.5873	5/2 <sup>+</sup>
												1.6223	19/2 <sup>-</sup>
23	1.688	$0.07 \pm 0.02$							1.659			1.689	11/2 <sup>-</sup> ; 9/2 <sup>-</sup>
						1.701	(2)	(0.078; 0.093)	1.689	5	3.7	1.701	(5/2 <sup>+</sup> ; 3/2 <sup>+</sup> )
24	1.714	$0.10 \pm 0.01$	0	1/2	0.016	1.731	0	0.026	1.714	0	0.012	1.714	1/2 <sup>+</sup>
25	1.758	$0.10 \pm 0.01$	0	1/2	0.016	1.777	0	0.021					
26	1.812	$0.055 \pm 0.006$	2	5/2; 3/2	0.042; 0.052	1.833	2	0.081; 0.095	1.779	1	0.027; 0.028	1.7618	3/2 <sup>-</sup> ; 1/2 <sup>-</sup>
27	1.822	$0.020 \pm 0.003$							1.813	2	0.064; 0.068	1.7743	11/2 <sup>-</sup>
28	1.839	$0.013 \pm 0.002$							1.825	2	0.075; 0.081	1.777 <sup>j</sup>	1/2 <sup>+</sup>
29	1.858	$0.013 \pm 0.002$							1.842	2	0.041; 0.043	1.825	5/2 <sup>+</sup> ; 3/2 <sup>+</sup>
									1.861	0	0.062	1.8434	5/2 <sup>+</sup> ; 3/2 <sup>+</sup>
									1.861	0	0.062	1.861	1/2 <sup>+</sup>
									1.878	2	0.25; 0.27	1.8622	15/2 <sup>+</sup>
						1.884			1.8801			1.8801	5/2 <sup>+</sup> ; 3/2 <sup>+</sup>
30	1.969	$0.067 \pm 0.010$	2	5/2; 3/2	0.049; 0.061	1.984	2	0.061; 0.071	1.893			1.936	1/2 <sup>+</sup>
									1.936	0	0.061	1.9615	
31	1.996	$0.35 \pm 0.02$	1	3/2; 1/2	0.09; 0.10				1.969	2	0.20; 0.21	1.9710	5/2 <sup>+</sup> ; 3/2 <sup>+</sup>
									1.997	2	0.12; 0.13	1.984 <sup>k</sup>	5/2 <sup>+</sup> ; 3/2 <sup>+</sup>
												1.9970	5/2 <sup>+</sup> ; 3/2 <sup>+</sup>
												2.0170	
												2.0175	1/2 <sup>+</sup>
32	2.068	$0.021 \pm 0.002$				2.076			2.057	0	0.076	2.057	
33	2.083	$0.02 \pm 0.01$				2.100			2.087			2.0634	
34	2.131	$0.18 \pm 0.02$				2.156			2.133	1	0.037; 0.039	2.0867	
												2.133	3/2 <sup>-</sup> ; 1/2 <sup>-</sup>

<sup>a</sup>Reference [18].<sup>b</sup>Reference [8].<sup>c</sup>Reference [6].<sup>d</sup>Integrated cross section (Levels 2 and 2').<sup>e</sup>Levels experimentally unresolved. Least squares fit in angular distribution.<sup>f</sup>Energy attributed to the  $l = 2$  component of unresolved doublet.<sup>g</sup>Integrated cross section ( $l = 2$  and  $l = 5$ ).<sup>h</sup>Level proposed to correspond to level 7.<sup>i</sup>Level proposed to correspond to level 19.<sup>j</sup>Level proposed to correspond to level 25.<sup>k</sup>Level proposed to correspond to level 30.

TABLE V. Experimental results for  $^{103}\text{Ru}$  from the  $^{104}\text{Ru}(d, t)$  reaction in comparison with previous transfer studies and the levels adopted by Nuclear Data Sheets. The asterisk denotes levels used in energy calibration.

Level number	Present work						$(d, t)^a$				$(p, d)^b$				Nuclear data <sup>c</sup>	
	$E_{\text{exc}}$ (MeV)	$[\sigma_{\text{exp}}(\theta)]_{\text{max}}$ (mb/sr)	$l$	$j$	$C^2S_{lj}$	$E_{\text{exc}}$ (MeV)	$l$	$C^2S_{lj}$	$E_{\text{exc}}$ (MeV)	$l$	$C^2S_{lj}$	$E_{\text{exc}}$ (MeV)	$J^\pi$	$E_{\text{exc}}$ (MeV)	$J^\pi$	
0	0.002	$3.80 \pm 0.02$	2	5/2	1.11	0.000	2	1.97	0.0054	2	1.29	0.00000	$3/2^+$	0.00000	$3/2^+$	
1	0.136*	$0.24 \pm 0.01$	2	5/2	0.072	0.133 (2)	(2)	(0.11; 0.14)	0.1356	2	0.13	0.136079	$5/2^+$	0.00281	$5/2^+$	
2	0.174*	$2.42 \pm 0.02$	0	1/2	0.29	0.171	0	0.43	0.1742	0	0.28	0.17426	$1/2^+$	0.136079	$5/2^+$	
3	0.213*	$0.31 \pm 0.03$	4	7/2	2.07	0.210	4	2.36	0.2128	4	0.96	0.21356	$7/2^+$	0.17426	$1/2^+$	
4	0.239	$0.20 \pm 0.02$	5	11/2	1.47	0.235	5	1.92	0.2397	5	1.55	0.2382	$11/2^-$	0.21356	$7/2^+$	
5	0.297*	$0.38 \pm 0.03$	3	7/2; 5/2	0.16; 0.22	0.294 (0)	(0)	(0.08)	0.2971	3	0.17	0.2971	$(7/2^-)$	0.2382	$11/2^-$	
6	0.346	$0.30 \pm 0.02$	2	5/2; 3/2	0.10; 0.13	0.343	2	0.16	0.3464	2	0.14	0.29748	$(3/2^+)$	0.2971	$(7/2^-)$	
7	0.406	$1.00 \pm 0.06$	2	5/2; 3/2	0.35; 0.44	0.402	2	0.62	0.4056	2	0.31; 0.34	0.34638	$3/2^+$	0.29748	$(3/2^+)$	
8	0.432*	$0.60 \pm 0.03$	0	1/2	0.070	0.428	0	0.12	0.4329	0	0.09	0.40415	$7/2^+$	0.34638	$3/2^+$	
9	0.501	$0.46 \pm 0.03$	2	5/2; 3/2	0.17; 0.20	0.497	2	0.26	0.5011	2	0.22	0.40608	$5/2^+; 3/2^+$	0.40415	$7/2^+$	
10	0.540	$0.145 \pm 0.013^d$	2	5/2; 3/2	0.21; 0.25	0.587	2	0.38	0.5930	2	0.21	0.6220	$(5/2^+; 3/2^+)$	0.59197	$(5/2^+)$	
11	0.548															0.545
12	0.556					0.5511 <sup>e</sup>	2	0.10		0	0.02	0.55458	$(1/2^+)$	0.55458	$(1/2^+)$	
13	0.592	$0.54 \pm 0.03$	2	5/2; 3/2	0.21; 0.25	0.587	2	0.38	0.6281	(2)	(0.05)	0.56817	$(9/2)$	0.5577	$(9/2)$	
14	0.662	$0.040 \pm 0.009$				0.658 (2)	(2)	(0.03; 0.04)	0.6630	2	0.05	0.56817	$(5/2^+; 3/2^+)$	0.56287	$(5/2^+; 3/2^+)$	
15	0.697	$0.04 \pm 0.01$				0.693	4	0.47	0.7012	4	0.34	0.56817	$(1/2^+)$	0.56817	$(1/2^+)$	
16	0.737	$0.71 \pm 0.05$	0	1/2	0.086	0.731	0	0.15	0.7388	0	0.09	0.59197	$(5/2^+)$	0.59197	$(5/2^+)$	
17	0.775	$0.28 \pm 0.10$	2	5/2; 3/2	0.11; 0.13							0.6220	$15/2^-$	0.6220	$(5/2^+)$	
18	0.855	$0.025 \pm 0.004$										0.6537	$15/2^-$	0.6537	$15/2^-$	
19	0.908	$0.108 \pm 0.008$	(2)	(5/2; 3/2)	(0.050; 0.061)	0.902	2	0.07	0.9039	2	(0.08; 0.09)	0.66155	$(3/2^+)$	0.66155	$(3/2^+)$	
20	0.928	$0.04 \pm 0.01$										0.6972	$9/2^+; 7/2^+$	0.6972	$9/2^+; 7/2^+$	
21	0.942	$0.040 \pm 0.005$										0.7352	$(5/2^+)$	0.7352	$(5/2^+)$	
												0.73689	$1/2^+$	0.73689	$1/2^+$	
												0.7488	$(5/2^+)$	0.7488	$(5/2^+)$	
												0.7741	$(11/2^+)$	0.7741	$(11/2^+)$	
												0.77477	$(5/2^+; 3/2)$	0.77477	$(5/2^+; 3/2)$	
												0.87371	$(5/2^+; 3/2^+)$	0.87371	$(5/2^+; 3/2^+)$	
												0.90305	$(< 5/2^+)$	0.90305	$(< 5/2^+)$	
												0.90536	$5/2^+; 3/2^+$	0.90536	$5/2^+; 3/2^+$	
												0.90764	$(< 5/2^+)$	0.90764	$(< 5/2^+)$	
												0.9116	$(7/2^+)$	0.9116	$(7/2^+)$	
												0.92724	$(3/2^+; 1/2^+)$	0.92724	$(3/2^+; 1/2^+)$	
												0.9313	$(5/2; 3/2)$	0.9313	$(5/2; 3/2)$	
												0.94050	$(3/2)$	0.94050	$(3/2)$	
												0.9544	$(3/2)$	0.9544	$(3/2)$	
												0.9916	$(3/2)$	0.9916	$(3/2)$	



TABLE V. (Continued).

Level number	Present work				$(d, t)^a$				$(p, d)^b$				Nuclear data <sup>c</sup>	
	$E_{\text{exc}}$ (MeV)	$[\sigma_{\text{exp}}(\theta)]_{\text{max}}$ (mb/sr)	$l$	$j$	$C^2S_{lj}$	$E_{\text{exc}}$ (MeV)	$l$	$C^2S_{lj}$	$E_{\text{exc}}$ (MeV)	$l$	$C^2S_{lj}$	$E_{\text{exc}}$ (MeV)	$J^\pi$	
37	2.022	0.114±0.013							1.96192			2.0037	(5/2 <sup>+</sup> ; 3/2 <sup>+</sup> )	
38	2.167	0.23±0.07	4	9/2; 7/2	1.6; 2.7				2.1319			2.132	19/2 <sup>+</sup> (23/2 <sup>-</sup> )	
39	2.217	0.039±0.005							2.20611			2.2236		
40	2.232	0.145±0.015												
41	2.299	0.24±0.02	1	3/2; 1/2	0.04; 0.05									
42	2.384	0.37±0.02	1	3/2; 1/2	0.07; 0.08									
43	2.444	0.13±0.03												
44	2.507	0.076±0.008	1	3/2; 1/2	0.013; 0.018									
45	2.520	0.155±0.015												

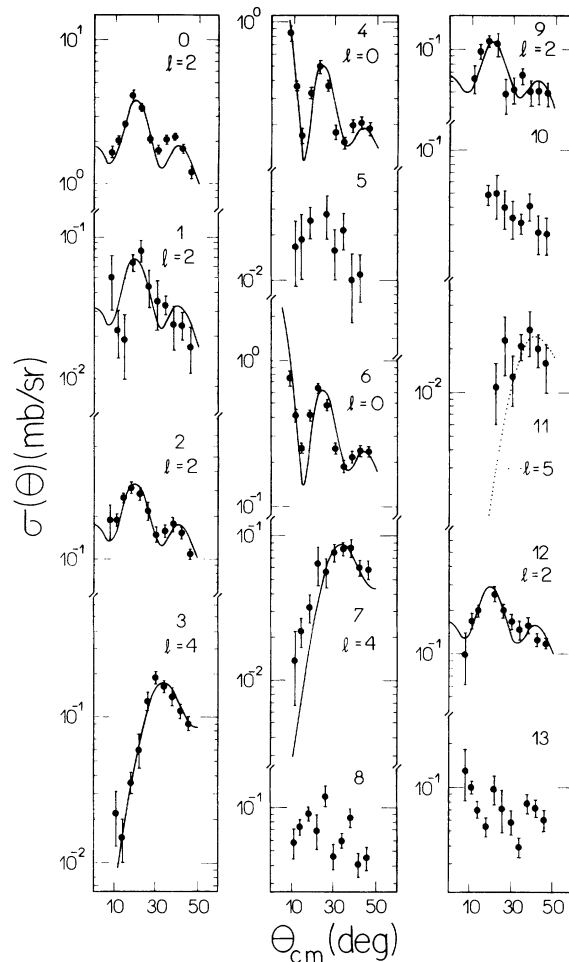
<sup>a</sup>Reference [19].<sup>b</sup>Reference [20].<sup>c</sup>Reference [7].

FIG. 2. Angular distributions for the  $^{100}\text{Ru}(d, t)^{99}\text{Ru}$  reaction in comparison with DWBA predictions. Error bars represent uncertainties due to statistics, plate scanning, and background (and/or contaminant) subtraction and do not include any error in the absolute cross section scale (see text).

definite  $l$  transfers, and the corresponding  $C^2S_{lj}$  values are also presented in Table III. This table also shows, for comparison, the levels adopted by the nuclear data compilation [5]. Additional levels, at 1.1184 and 1.29078 MeV reported by Whisnant *et al.* [17], are also presented in columns 7 and 8. Although no clear discrimination between  $l = 4$  and  $l = 5$  is allowed by the data, the level excited at 1.072 MeV is supposed to be the known  $11/2^-$  state. An  $l = 3$  transition was searched for, in particular at 1.291 MeV, where a ( $^3\text{He}, 2n\gamma$ ) work [17] located a ( $7/2^-$ ) level, but was not observed above the detection limit.

### B. The $^{102}\text{Ru}(d, t)^{101}\text{Ru}$ reaction

In this experiment a detection limit of only  $3 \mu\text{b/sr}$  could be achieved in the excitation energy region below 2.2 MeV, due to a relatively clean target. Table IV shows the present results in comparison with a ( $p, d$ ) study by Dickey *et al.* [18], which has a poorer energy resolution



of only 24 keV. Also the results of the  $(d, p)$  work of this group [8] and the adopted levels [6] are tabulated. In Fig. 3 the experimental angular distributions are displayed together with DWBA predictions.

The level energies in Table IV were determined with standard deviations of less than 2 keV for all levels below 1.9 MeV and no more than 3 keV above this energy. The difference between the attributed excitation energies and the adopted ones is always smaller than 2 keV, where identification with levels based on  $\gamma$ -ray results is unambiguous. Also, agreement between the excitation energies obtained in the present  $(d, t)$  and the former  $(d, p)$  work [8] is excellent. On the other hand, the results of the previous  $(p, d)$  study [18] are clearly affected by a systematic discrepancy with respect to both, the  $(d, t)$  and  $\gamma$ -ray information. The excitation energy difference is of the order of  $+(10-20)$  keV, starting at about 1 MeV, as is evidenced especially through the comparative analysis of the stronger transitions detected in both pick-up studies. The worst case is the level 19 where  $+33$  keV of energy shift is verified. Thus, several levels presented in

the recent nuclear data compilation [6], which are based exclusively on information by Dickey *et al.* [18], should have their excitation energies revised.

General agreement between neutron hole spectroscopic strength extracted in the present  $(d, t)$  and in the former  $(p, d)$  [18] works is observed. Specific comments on the experimental results are made in the following.

Level 1 lies below the detection limit, except at the 3 angles around the maximum for  $l = 2$  transfer, thus the value of  $C^2S_{d_{3/2}}$  between parenthesis is an estimate. Peaks numbered 17, 27, 28, 29, 32, and 33 were also only observed at  $\theta_{\text{lab}} = 10^\circ, 22^\circ,$  and  $28^\circ$  and, since they do not correspond to levels with known spins and parities, only excitation energies are reported. Peaks 2 and 2' could not be adequately separated by the peak fitting routine and the  $l = 4$  and  $l = 2$  contributions were extracted through a least-squares fit on the integrated angular distribution, as shown in Fig. 3. Peak 5 is dominated by the strong  $l = 2$  transition at 0.535 MeV and the  $l = 5$  contribution was also obtained by the same fitting procedure, the extracted  $C^2S_{h_{11/2}}$  being uncertain

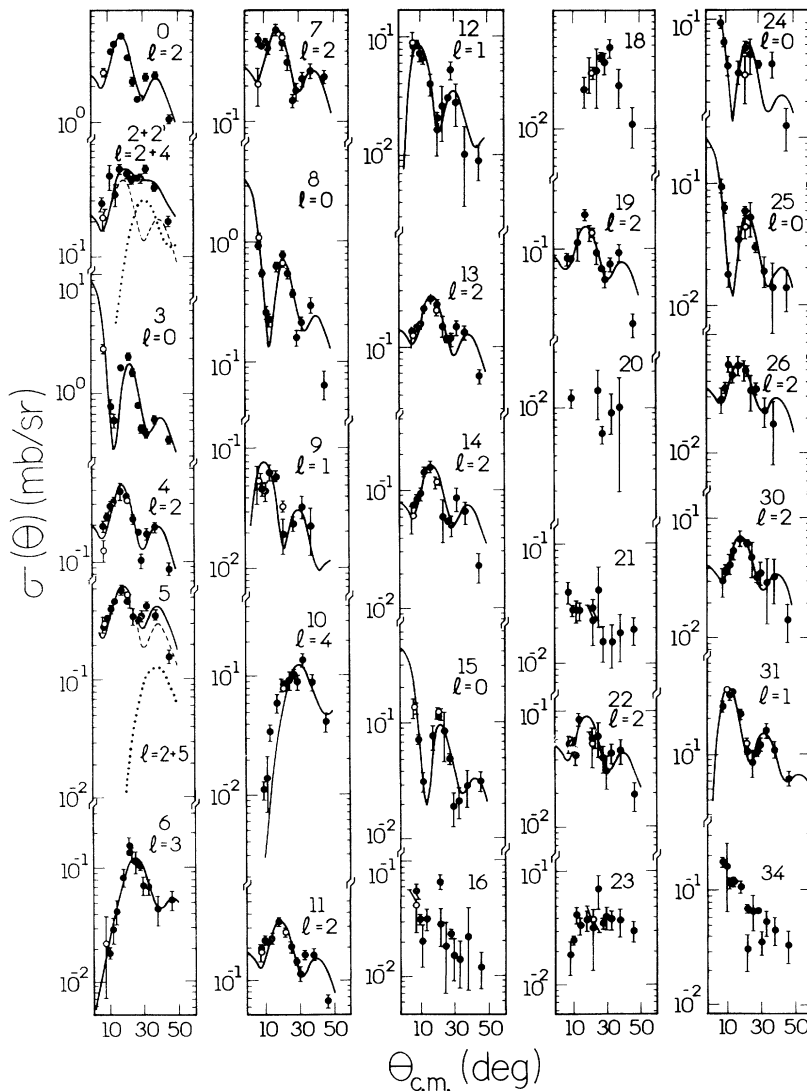


FIG. 3. Angular distributions for the  $^{102}\text{Ru}(d, t)^{101}\text{Ru}$  reaction in comparison with DWBA predictions. See caption of Fig. 2.

to 25%.

Level 6 corresponds in energy to the  $l = 3$  transition seen in  $(d, p)$  [8] and is very well characterized by the same orbital angular momentum transfer. Dickey *et al.* [18] could not resolve this state, present as a shoulder in the published spectrum, from the neighboring  $l = 2 + l = 0$  transitions at 0.615 and 0.622 MeV, which they also could not separate. So, the level at 0.623 MeV with  $J^\pi = 5/2^+, 3/2^+$ , indicated in the nuclear data tabulation [6] as measured by Dickey *et al.* [18], is already represented by the adopted level at 0.6163 MeV,  $J^\pi = (5/2^+, 3/2^+)$  and should be excluded.

Level 9 is, in  $(d, t)$ , better described as  $l = 1$  transfer (see Fig. 3) than as the  $l = 2$  previously attributed in  $(p, d)$  [18] and  $(d, p)$  [8]. The attributions may thus be open to questioning. At 0.719 MeV, level 10 corresponds predominantly to  $l = 4$  in the present work and  $(p, d)$  [18]. A closer inspection shows, however, that the agreement with the DWBA prediction at forward angles is subtly worse than for other typical  $l = 4$  transfers. In the angular distribution obtained in  $(p, d)$ , this effect is substantially enhanced and could signify an additional  $l = 1$  transfer being detected. In fact, the  $(d, p)$  reaction located at 0.718 MeV an  $l = 1$  transfer, which only through severe contamination at the forward angles, could be associated to an  $l = 4$  transfer. It seems thus that two levels with different characteristics are being preferentially populated in the pick-up and stripping reactions. Dickey *et al.* [18] did, in fact, not attribute any  $l = 1$  transfer in their work. The inspection of the angular distribution associated to the state at 0.927 MeV, which Dickey *et al.* [18] report as populated by  $l = 2$ , also shows a behavior that is not in disagreement with an  $l = 1$  transfer. Thus, this state is tentatively identified with the level at 0.907 MeV seen in the present study and already adopted as  $3/2^-, 1/2^-$  by Nuclear Data Sheets [6]. No transition to the level at 1.225 MeV, reported in the  $(p, d)$  work [18], was observed above the detection limit. Level 17 was seen at only three angles, but the data available, although compatible with an  $l = 2$  transfer, exclude an  $l = 0$  character. This level should thus correspond to the 1.268 MeV reported by the  $(d, p)$  work, but not to the 1.276 MeV level by Dickey *et al.* [18]. A clear  $l = 1$  transition was detected to the level 31, in apparent disagreement with the experimental findings of the  $(d, p)$  study [8], which reports an  $l = 2$  transfer. The  $(d, p)$  angular distribution is, however, compatible with an  $l = 1$  transfer due to the absence of data at scattering angles smaller than  $20^\circ$ . In this case, the extracted reduced spectroscopic factor,  $C^2 S'_{ij}$ , should be 0.04 and spin and parity of the correspondent level should be revised.

### C. The $^{104}\text{Ru}(d, t)^{103}\text{Ru}$ reaction

This experiment extended the excitation energy interval analyzed by pick-up reactions up to 2.6 MeV. The detection limit was  $10 \mu\text{b}/\text{sr}$ , due to a relatively thin target, somewhat more contaminated during evaporation. Previous pick-up studies [19,20], including a  $(d, t)$  work

[19], did not exceed 0.9 MeV of excitation energy. Their results are presented in Table V in comparison with the present ones and with the adopted levels [7]. The work of Berg *et al.* [20] was performed at a high dispersion spectrograph with 5–8 keV of resolution and studied both the  $(p, d)$  and  $(d, p)$  reactions leading to  $^{103}\text{Ru}$ , unfortunately with very poor statistics. They ascertained that the stripping reaction populates preferentially the ground state, while pick-up selects the known state [7] at 2.81 keV, associated by them to their level at 5.4 keV. In the present work the excitation energy of level 0, as obtained from the internal calibration with the levels marked with an asterisk, is  $2 \pm 1$  keV and thus confirms the predominant excitation of the first excited level in pick-up. Inspection of Table V reveals excellent agreement between the level energies here obtained and all those of both previous pick-up studies.

The comparison of the extracted spectroscopic strengths with those reported for the same reaction at 17 MeV by Diehl *et al.* [19] shows general agreement for the relative values, although the absolute values of the older work are systematically higher. The lack of finite range and nonlocality corrections in the older DWBA calculation can be responsible for part of the discrepancy. Diehl *et al.* [19] also did not publish the geometry of the potential that binds the transferred neutron, another known source of differences in absolute values. The results of the  $(p, d)$  work of Berg *et al.* [20] are, on the other hand, in good agreement with the present ones, exception made to the first  $l = 2$  and the lowest  $l = 4$  excitations, where the discrepancies of up to a factor of two are directly related to the reported cross sections and cannot be attributed to analysis.

Figure 4 displays the angular distributions obtained in this work and, in the following, comments on some specific attributions are made.

Level 5, at 0.297 MeV, is a clear  $l = 3$  transition. The misattribution in the  $(d, t)$  work of Diehl *et al.* [19] may have been caused by the lack of data at forward angles, crucial to distinguish the correct value from  $l = 0$ . Berg *et al.* [20] also attribute  $l = 3$  to this transition. A triplet of levels (10, 11, and 12) could be clearly resolved where Diehl *et al.* [19] located an  $l = 1$  transition, but separated angular distributions were not obtained. Berg *et al.* [20] who also analyzed integrated cross sections, decided for a superposition of  $l = 2$  and  $l = 0$  transfer in this energy region, on a rather structureless experimental angular distribution. The present data are not sufficient for deciding on the divergence exposed, because of contamination at  $\theta = 8^\circ$ . The cross section associated to level 15 was at crucial forward angles near the detection limit, but if an  $l = 4$  transfer is supposed the  $C^2 S_{ij}$  value would be compatible with other studies.

Above level 20 all information is new and the identification with levels adopted by the nuclear data compilation [7] is tentative. Attention is drawn especially to the observation of an intense  $l = 4$  excitation at 2.167 MeV and of three clean  $l = 1$  transfers around 2.4 MeV, besides the lower  $l = 1$  at 1.756 MeV. Another ( $l = 4$ ) and several  $l = 2$  transitions are also reported for the first time. Relatively strong excitations (peaks 30 and 31) at

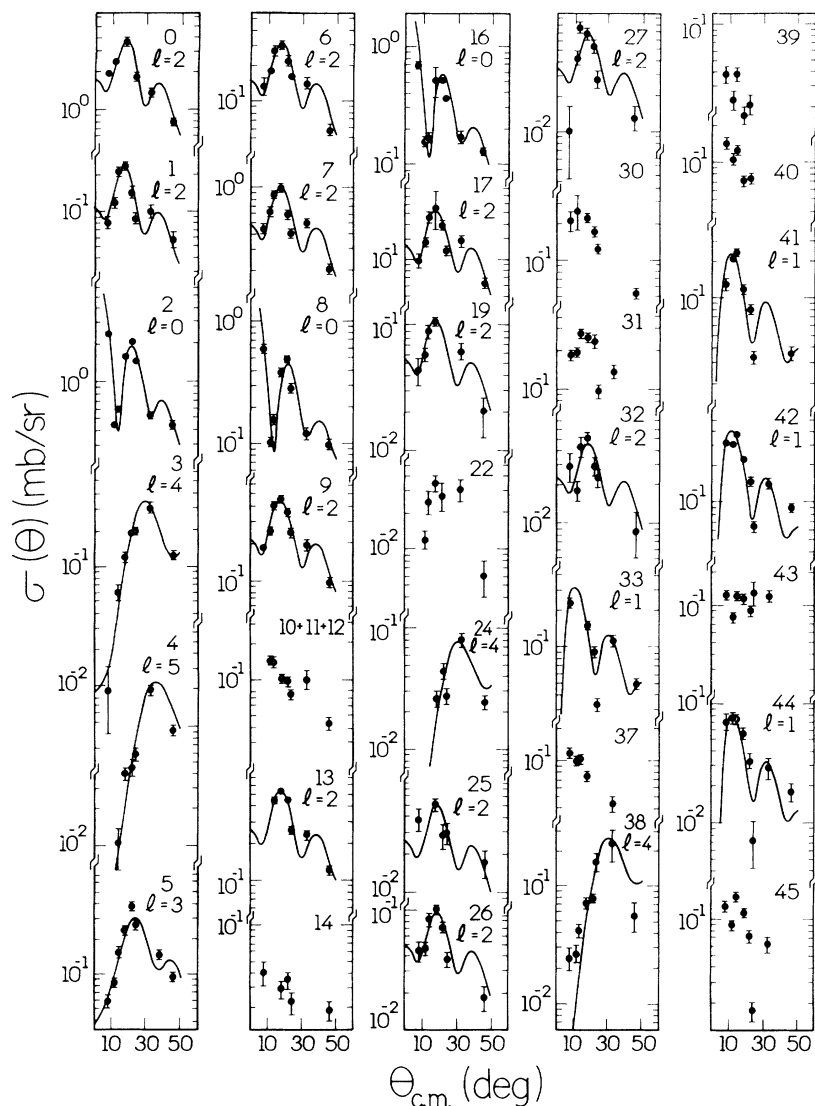


FIG. 4. Angular distributions for the  $^{104}\text{Ru}(d, t)^{103}\text{Ru}$  reaction in comparison with DWBA predictions. See caption of Fig. 2.

1.403 and 1.491 MeV correspond to forward peaked angular distributions, but cannot be clearly identified. If associated to  $l = 2$  transfer, their summed spectroscopic strength would amount to  $C^2S_{d_{5/2}} \sim 0.3$ . Peaks 28 and 29 are also relatively intense and their angular distributions, not shown in Fig. 4 since represented by less than five data points, show maxima at respectively  $\theta = 18^\circ$  and  $12^\circ$  and, if corresponding to  $l = 2$  and  $l = 1$ , respectively, would mean additional  $C^2S_{l_j}$  of  $\sim 0.04$  and  $\sim 0.04$ .

#### IV. DISCUSSION

For comparative appreciation, Fig. 5 displays, as bars, the observed spectroscopic strengths as a function of excitation energy for the three Ru isotopes under investigation and for the several  $l$  transferred (taken where the level spin is not known, as associated to  $j = l + 1/2$ ). An arrow indicates, for each nuclide, the maximum excitation energy scanned. An overall similarity may be noted, but for all  $l$  transfers the strengths tend to be located

at progressively lower excitation energies as the neutron number is increased.

Most of the detected strength is, as expected, associated to even  $l$  values. The principal  $l = 0$  excitations are found below 0.8 MeV and correspond to at most three levels. It can be stated that, since the detection limit for  $l = 0$  is low, no important fragmentation occurs. For all studied isotopes the by far strongest  $l = 2$  component is located at the first  $5/2^+$  level (note the scale factor of 1/4 for these bars). The remaining detected  $l = 2$  strength is for  $^{101,103}\text{Ru}$  spread among several levels in a wide energy range. In  $^{99}\text{Ru}$ , on the other hand, at most five states with  $l = 2$  characteristics were observed. Very similar and intense  $l = 4$  transfers are associated to the first known  $7/2^+$  levels below 0.4 MeV in all three isotopes, while the first known  $9/2^+$  states appear with one fourth of that strength at  $\sim 0.7$  MeV in  $^{99,101}\text{Ru}$ . Several levels which could, in principle, be excited by  $l = 4$  transfer are known, from other reactions or decay, in all three isotopes (see Tables III, IV, and V), but are populated below the detection limit (in the worst case  $C^2S_{g_{7/2}} = 0.4$ ). Attention is to be called to the first observation in  $^{103}\text{Ru}$  of a

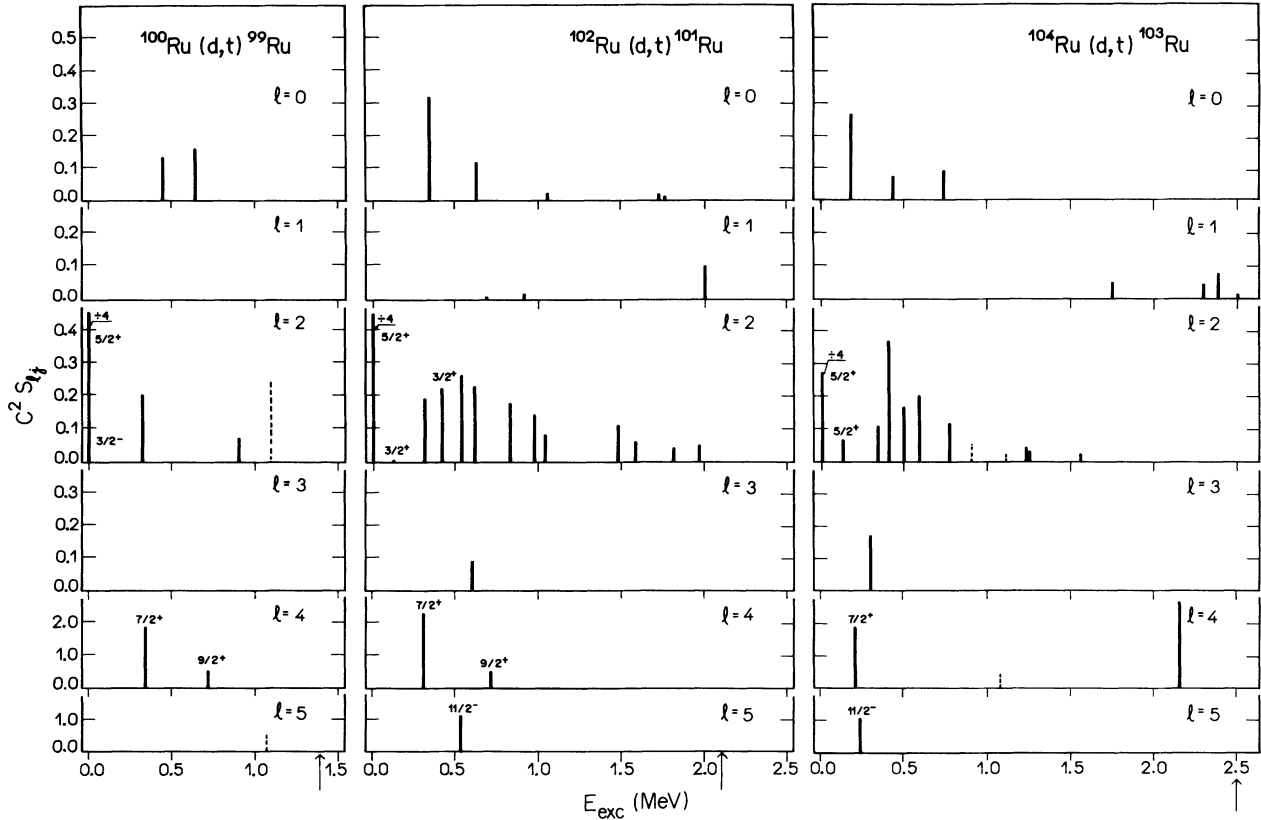


FIG. 5. Spectroscopic strength distributions, organized as functions of  $l$  transfer and excitation energy, obtained from the one neutron pick-up reactions indicated. Note the reduction factors for the strongest  $l = 2$  transitions. Tentative attributions are shown as broken bars and known spins (Refs. [5–7]) are marked. Where spins are not known, bars represent the spectroscopic strength associated to  $j = l + 1/2$ , exception made to the level at 2.2 MeV in  $^{103}\text{Ru}$ , excited through  $l = 4$ , which was taken as  $7/2^+$ .

state with clear and strong  $l = 4$  characteristics at 2.167 MeV. In fact, this  $l = 4$  excitation would correspond to  $C^2 S_{g_{7/2}} = 2.7$ , even higher than the intensity to the first  $7/2^+$  state, if this spin value should prevail.

With respect to the levels excited by an odd  $l$  transfer, no  $l = 1$  was seen in  $^{99}\text{Ru}$  below 1.5 MeV and all the important strengths seen in  $^{101,103}\text{Ru}$  lie above 1.7 MeV. Also no  $l = 3$  strength was located in  $^{99}\text{Ru}$  above the detection limit of  $C^2 S_{f_{7/2}} = 0.04$ , while the  $l = 3$  excitation seen at 0.597 MeV in  $^{100}\text{Ru}(d,p)^{101}\text{Ru}$  was confirmed and also  $l = 3$  was definitely associated to the level at 0.297 MeV in  $^{103}\text{Ru}$ . It is extremely interesting to note that no other, besides these very low-lying,  $l = 3$  excitations were detected up to, respectively, 2.2 and 2.5 MeV in  $^{101,103}\text{Ru}$ , which clearly demonstrates the singular character of these levels. The  $l = 3$  strength was, thus, located with higher intensity at progressively lower energy with increasing neutron number, if the  $7/2^-$  level at 1.291 MeV in  $^{99}\text{Ru}$  (Ref. [17]) is supposed undetected by experimental limitations. The  $l = 5$  strength, also located in a single level, decreases in energy in a similar way. For  $l = 5$  excitations the detection limit corresponds in the worst case, to  $C^2 S_{h_{11/2}} = 0.5$ .

It has long been established that one nucleon transfer reactions, especially if well-known light projectiles are

employed, result in clean spectroscopic informations of two kinds. On one side, a global view of the spectroscopic strengths is associated to occupation and vacancy of shell-model orbitals in the ground state of the target nucleus. Such information is systematized in Table VI for the occupancy data extracted in this work and will be further discussed below. On the other side, specific states in the residual nucleus may have their quasiparticle character defined, especially if results of the complementary stripping or pick-up reactions are also available. Figure 6, later presented, will be used to point these aspects out.

In Table VI the summed spectroscopic strength of excitations which could be associated without doubt to each  $l$  transfer is shown for the three target nuclei investigated. The column labelled  $1g$  presents only the strength which can with certainty be attributed to the  $1g_{7/2}$  orbital. Thus the population of  $9/2^+$  levels, hole states in the  $N = 50$  core in  $^{99,101}\text{Ru}$ , and of a state of unknown spin at 1.08 MeV in  $^{103}\text{Ru}$ , all with  $C^2 S_{g_{9/2}} \sim 0.5$ , was not considered in this table. The total detected  $l = 1$  and  $l = 3$  strengths are shown, respectively, in columns 3 and 5, under the hypothesis that states associated to the next major shell are excited. This assumption will be fundamented, with basis on  $(d,p)$  results, in the further

TABLE VI. Sums of the one neutron pick-up spectroscopic strength associated to each  $l$  value for  $^{100,102,104}\text{Ru}$ . The last column indicates the total spectroscopic strength associated with certainty to the 50–82 neutron shell (see text).

Target nucleus	$\sum C^2S$						Total spectroscopic strength
	3s	3p	2d	2f	1g	1h	
$^{100}\text{Ru}$	0.29	0.00	2.30	0.00	1.8	0.6	5.0
$^{102}\text{Ru}$	0.49	0.10	3.36	0.09	2.3	1.2	7.4
$^{104}\text{Ru}$	0.45	0.17	2.23	0.16	2.1 (4.8)	1.5	6.3 (9.0)

discussion. For the  $l = 2$  transfers, when the final  $j$  is not known, the strength for  $j = l + 1/2$  was arbitrarily taken. If this choice should prove incorrect for all those levels, the summed spectroscopic strength would increase by at most 5%, 10%, and 10% for  $^{100,102,104}\text{Ru}$ , respectively. For the  $^{104}\text{Ru}$  nucleus, if the  $l = 4$  excitation at 2.167 MeV could be characterized as an  $1g_{7/2}$  contribution, the values indicated in parenthesis result. The last column of Table VI presents thus the total summed spec-

troscopic strength which is with certainty associated to the 50–82 shell, the  $3p$  and  $2f$  transfers being excluded.

The present results make it clear that in the reactions studied most of the strength was found. In fact, if the  $N = 50$  core could be considered closed,  $^{100,102,104}\text{Ru}$  should correspond, respectively, to 6, 8, and 10 valence neutrons. For  $^{104}\text{Ru}$  the total spectroscopic strength detected would percentually be similar to those of the other two isotopes studied, if the value in parenthesis is con-

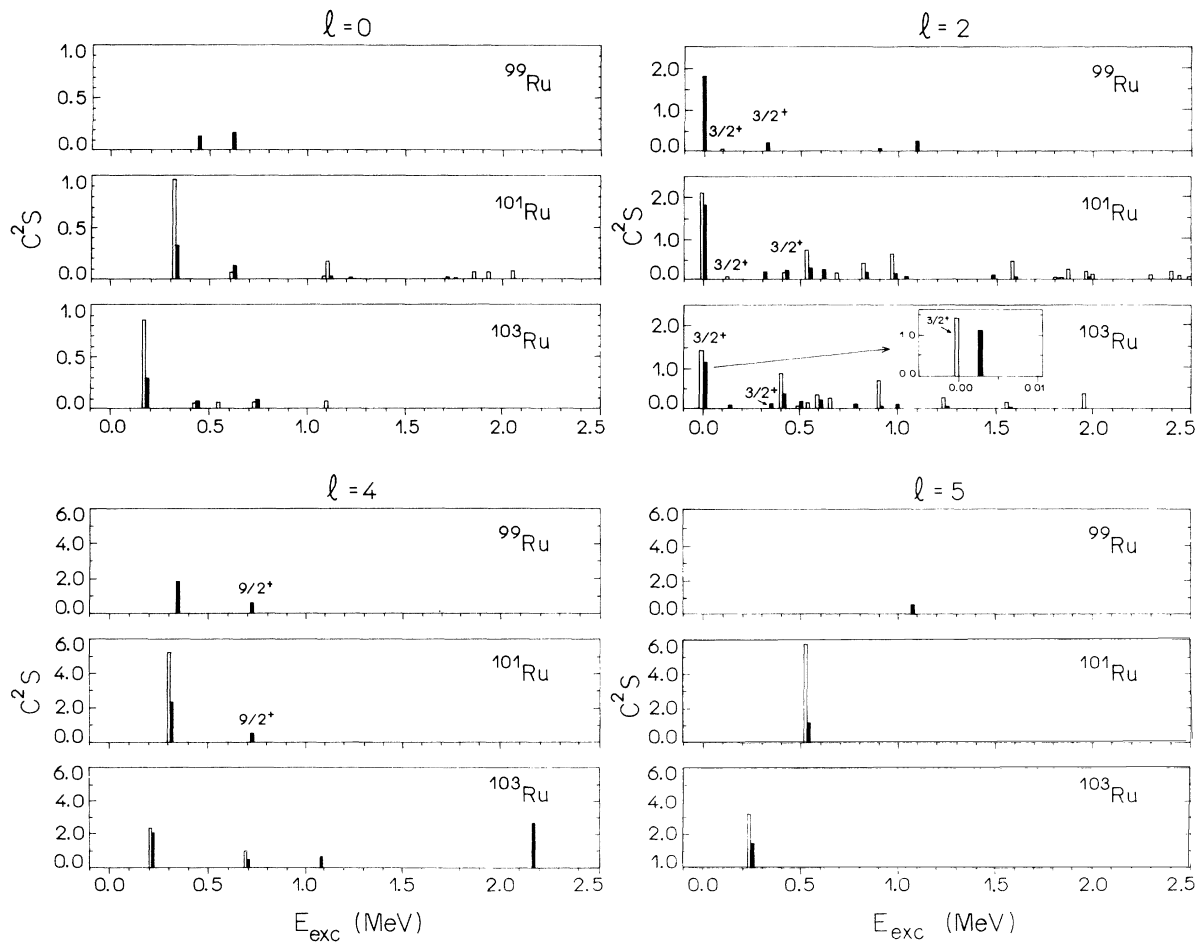


FIG. 6. Hole (represented as solid bars) and particle (represented as open bars) strengths as a function of excitation energy and  $l$  transfer in  $^{99,101,103}\text{Ru}$ . The particle strength was taken from Duarte *et al.* (Ref. [8]) for  $^{101}\text{Ru}$  and Fortune *et al.* (Ref. [21]) for  $^{103}\text{Ru}$ , up to 2.0 MeV, and for  $^{99}\text{Ru}$  there is no experimental information. Hole strength is represented to the right of the excitation energy of the respective level while the particle strength is represented to the left. Note the inset for the two first levels excited by  $l = 2$  in  $^{103}\text{Ru}$ .

sidered. A global view of Table VI demonstrates that the neutron hole strength is widely spread among all the spherical shell-model valence orbitals. If exception is possibly made to the  $1g_{7/2}$  orbital in  $^{104}\text{Ru}$ , none other is seen to concentrate more than about one-third of the respective sum rule limit and no filling pattern with increasing  $N$  emerges. The missing strength of only about  $\sum C^2S = 1.0$  in each isotope (if the value in parenthesis is taken) is not expected to disrupt this picture.

Figure 6 displays, in addition to the present results, also the spectroscopic strengths [taken as  $C^2S'_{lj} = C^2(2j+1)S_{lj}$ ] for the  $^{100,102}\text{Ru}(d,p)$  reactions [8,21]. For better comparative visualization, the same scales are employed for each  $l$  transfer for the three isotopes. It is to be noted that absolute values are presented for  $C^2S'_{lj}(d,p)$  and  $C^2S_{lj}(d,t)$  and that the maximum values on scale are about  $(2j+1)/2$ . Levels with known  $J^\pi$  of  $3/2^+$  and  $9/2^+$  are marked. Inspection of Fig. 6 demonstrates that, as expected on simple lines, most of the levels strongly excited in the pick-up reactions are also in the corresponding stripping reactions. An exception is the known  $9/2^+$  level at 0.7 MeV in  $^{101}\text{Ru}$ , which was not detected in  $^{100}\text{Ru}(d,p)$ . This is not surprising for  $1g_{9/2}$  states, since they should correspond to a totally occupied orbital in the  $N = 50$  core. The nonobservation in  $^{102}\text{Ru}(d,p)$  of the level excited at 1.1 MeV in  $^{104}\text{Ru}(d,t)$  with a strength similar to that of the above mentioned one in  $^{102}\text{Ru}(d,t)$ , makes it a candidate for also being a  $9/2^+$  state. Even if no  $(d,p)$  information is available for  $^{99}\text{Ru}$ , by comparison with the other two isotopes, a similar pattern seems to emerge. In particular, there also exists a  $9/2^+$  level at 0.7 MeV in  $^{99}\text{Ru}$  and the most important  $l = 4$ ,  $l = 2$ , and  $l = 0$  excitations have their counterparts in  $^{101}\text{Ru}$ . The overall similarity prevails also with  $^{103}\text{Ru}$ . Two important exceptions should, however, be focused: As already pointed out, the ground state of  $^{103}\text{Ru}$ , preferentially excited in  $(d,p)$ , is not so in  $(d,t)$ , where, in turn, a predominant population of the  $5/2_1^+$  level at 3 keV is observed (note the amplified energy scale in the inset of Fig. 6) and no excitation similar to the  $(7/2, 9/2)^+$  state at 2.2 MeV seems to exist at least in  $^{101}\text{Ru}$ . It is to be regretted that the  $^{102}\text{Ru}(d,p)$  reaction by Fortune *et al.* [21], which could help to define the spin of this state, did not cover excitation energies above 2.0 MeV.

Concerning odd  $l$  transfers, not much experimental information is available. The strong  $l = 5$  excitations detected are associated to known  $11/2^-$  levels and show, as expected, increasing hole character as  $N$  is augmented. No fragmentation was observed, although it should be remembered that the detection limit for  $l = 5$  is relatively high. The  $l = 1$  strength seen in the present  $(d,t)$  work for  $^{101,103}\text{Ru}$ , being perhaps undetected in  $^{99}\text{Ru}$  by experimental limitations, lies mostly in the higher excitation energy region. Although  $l = 1$  excitations are also seen in  $^{100}\text{Ru}(d,p)$  (Ref. [8]), no clearcut relation with the  $(d,t)$  results is established and the most intense  $l = 1$  transfers observed in  $^{104}\text{Ru}(d,t)$  lie outside the energy interval analyzed in the corresponding  $(d,p)$  reaction. As for the challenging low-lying  $l = 3$  levels, they are stronger excited in  $(d,p)$  than in  $(d,t)$ , especially in the case of the 0.6 MeV state in  $^{101}\text{Ru}$ , where the fac-

tor between  $C^2S'_{lj}$  and  $C^2S_{lj}$  (see columns 12 and 6 of Table IV) is about seven. This information was taken as indicative that these states are not core excitations of the  $1f$  orbital.

Figure 7 displays the excitation energy of the levels populated through  $l = 3$ , taken as  $7/2^-$ , and of possibly related levels in  $^{99}\text{Ru}$  (Ref. [17]) and  $^{105}\text{Ru}$  (Ref. [22]) as a function of mass number, together with that of the known  $11/2^-$  states. A relationship of the  $l = 3$  and  $l = 5$  excitations seems clear and may be of the same origin as that exposed for  $^{99}\text{Ru}$  by the particle plus rotor Coriolis coupled calculations of Whisnant *et al.* [17], although conflicting data in the literature open room for controversies [8]. Figure 7 also illustrates the relative constancy of the excitation energy of the first  $7/2^+$  levels, which also appear to have a quite peculiar character, not being influenced by the progressive addition of neutrons to the  $N = 50$  core. Also shown in the figure are the excitation energies of the first  $2^+$  and  $3^-$  states in the even ruthenium isotopes. It is to be noted that the  $3^-$  levels, normally referred to as octupolar vibrations associated to a coherent superposition of particle-hole pairs in adjacent shells and therefore less affected by neutron filling, go down in energy by 0.5 MeV from  $^{98}\text{Ru}$  to  $^{104}\text{Ru}$ , even more than the  $2_1^+$  states, formerly supposed as characterizing increasing quadrupolar deformation.

It is, on the other hand, also amazing to recall that, although the spectroscopic strength seen in the transfer reactions on the even target isotopes is widely spread among the several orbital angular momenta associated to the 50 to 82 shell, for each  $l$  value, as may be appreciated in Fig. 6, the pick-up reactions under study clearly select, for very preferential population, one, or at most a few, state(s) of the final nuclei with neat quasiparticle character. This excitation pattern is not expected if the Ru isotopes were simple rigid rotors with deformations cor-

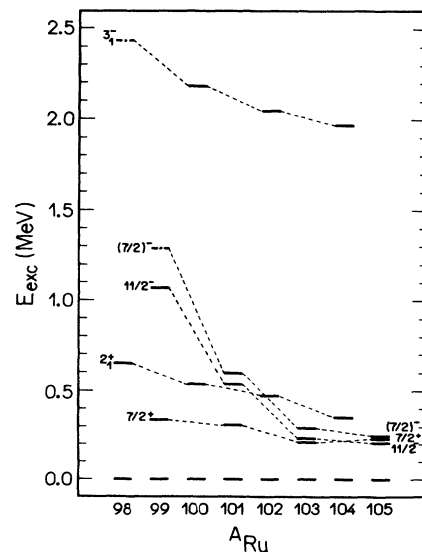


FIG. 7. Excitation energies of the  $7/2_1^+$ ,  $11/2_1^-$ , and  $(7/2)_1^-$  states for the odd isotopes and of the  $2_1^+$  and  $3_1^-$  levels for the even isotopes of Ru, as a function of mass number.

responding to the experimentally determined [23,24]  $\beta_2$ , which range between 0.21 and 0.27 for  $^{100}\text{Ru}$  to  $^{104}\text{Ru}$ . In fact, if the expansion coefficients of states in a statically deformed well onto a spherical basis, as calculated by Chi [25], are analyzed for each transferred  $l$  and  $j$ , it is verified that an important splitting should occur, especially between the several deformed states which originate from the same spherical orbital [26]. For this range of  $\beta_2$ , Coriolis coupling is not supposed to completely alter the picture [27]. A simple statically deformed core with a deformation parameter of about 0.2 being experimentally discarded, the necessity to resort to variable moment of inertia (VMI) procedures in the rotor analysis by Whisnant *et al.* [17] may reflect the need of relaxing this condition. It is also worthwhile to note that all model calculations [17,28] for the odd ruthenium isotopes with rotor ingredients had, in order to obtain accord, to adhere to  $\beta_2$  values smaller, by about a factor of two, than those experimentally determined for the even cores. An additional complicator may arise if the recently disclosed hexadecapolar degree of freedom [29] is to be considered.

Perhaps interacting boson-fermion model (IBFM) calculations, which are able to intrinsically absorb a certain softness and, if needed, also collectivity associated with multipolarities of higher order, could provide systematically more consistent results. However, the two existing IBFM studies do not publish spectroscopic factors for the complete chain of Ru isotopes, presenting pick-up results only on  $^{104}\text{Ru}$  (Ref. [30]) and  $^{102}\text{Ru}$  (Ref. [31]), both below 1.1 MeV. Furthermore, these two calculations only present spectroscopic factors associated to valence or-

bitals for  $^{103}\text{Ru}$ , being the information further restricted to positive parity ones in  $^{101}\text{Ru}$ . Thus, the challenging low-lying  $l = 3$  and  $l = 1$  states cannot have their properties confronted with theory. As far as their predictions go, Arias *et al.* [30] and Maino *et al.* [31] were able to appoint the general trends for the strength distributions, respectively, for the hole states in  $^{103}\text{Ru}$  and  $^{101}\text{Ru}$ , but could not reproduce the spreading, especially of the  $l = 2$  strength. Both works concentrate important  $l = 4$  strength in the first  $7/2^+$  levels, in accordance with experiment. Besides this, in  $^{103}\text{Ru}$ , Arias *et al.* [30] only foresee a second  $7/2^+$  state at 1.1 MeV to be populated by pick-up with a relatively small spectroscopic factor, but this state seems to correspond to a level seen in  $(d, t)$  and  $(d, p)$  at 0.7 MeV and certainly not to the strong  $l = 4$  excitation, observed at 2.2 MeV. As previously argued, it is felt that the interpretation of this excitation pattern and of the low-lying odd parity states, in addition to the rest of the systematic experimental information put into evidence by the present work, could represent a quite stringent test on the premises of this or other nuclear models.

#### ACKNOWLEDGMENTS

This work was partially supported by CNPq (Conselho Nacional do Desenvolvimento Científico e Tecnológico-Brasil), FINEP (Financiadora de Estudos e Projetos), and FAPESP (Fundação de Amparo à Pesquisa do Estado de São Paulo) and this is gratefully acknowledged.

- 
- [1] G. R. Satchler, *Direct Nuclear Reactions* (Clarendon, Oxford, 1983).
  - [2] A. Bohr and B. R. Mottelson, *Nuclear Structure* (Benjamin, New York, 1969, 1975), Vols. 1 and 2.
  - [3] J. M. Eisenberg and W. Greiner, *Microscopic Theory of the Nucleus* (North Holland, Amsterdam, 1972).
  - [4] *Nuclear Structure of the Zirconium Region*: Proceedings of International Workshop, Bad Honnef, edited by J. Ebert, R. A. Meyer, and K. Sistemich (Springer, Berlin, 1989).
  - [5] H. W. Müller and Chmielewska, Nucl. Data Sheets **48**, 663 (1986).
  - [6] J. Blachot, Nucl. Data Sheets **45**, 701 (1985); **63**, 305 (1991).
  - [7] D. de Frenne, E. Jacobs, and M. Verboven, Nucl. Data Sheets **45**, 363 (1985); J. Blachot, *ibid.* **68**, 311 (1993).
  - [8] J. L. M. Duarte, L. B. Horodyski-Matsushigue, T. Borello-Lewin, and O. Dietzsch, Phys. Rev. C **38**, 664 (1988).
  - [9] K. Koide, F. C. Sampaio, E. M. Takagui, J. H. Hirata, and O. Dietzsch, Nucl. Instrum. Methods **215**, 61 (1983).
  - [10] D. Pulino, G. M. Sipahi, G. M. Ukita, T. Borello-Lewin, L. B. Horodyski-Matsushigue, J. L. M. Duarte, W. G. P. Engel, and J. C. de Abreu, Rev. Bras. Apl. Vácuo, **10**, 87 (1991).
  - [11] C. M. Perey and F. G. Perey, Phys. Rev. **132**, 755 (1963).
  - [12] J. M. Lohr and W. Haerberli, Nucl. Phys. **A232**, 381 (1974).
  - [13] W. W. Daehnick, J. D. Childs, and Z. Vrcelj, Phys. Rev. C **21**, 2235 (1980).
  - [14] P. D. Kunz, DWUCK4 code, University of Colorado, 1974 (unpublished).
  - [15] F. G. Becchetti and G. Greenlees, Phys. Rev. **182**, 1190 (1969).
  - [16] R. H. Bassel, Phys. Rev. **149**, 791 (1966).
  - [17] C. S. Whisnant, K. D. Carnes, R. H. Castain, F. A. Rickey, G. S. Samudra, and P. C. Simms, Phys. Rev. C **34**, 443 (1986).
  - [18] S. A. Dickey, J. J. Kraushaar, and M. A. Rumore, J. Phys. G **12**, 745 (1986).
  - [19] R. C. Diehl, B. L. Cohen, R. A. Moyer, and L. H. Goldman, Phys. Rev. C **1**, 2085 (1970).
  - [20] G. P. A. Berg, M. Demartean, A. Hardt, H. Hürlimann, S. A. Martin, J. Meissburger, W. Oerlert, H. Seyfarth, B. Styczen, M. Kohler, I. Oelrich, and J. Scheerer, Nucl. Phys. **A379**, 93 (1982).
  - [21] H. T. Fortune, G. C. Morrison, J. A. Nolen Jr., and P. Kienle, Phys. Rev. C **3**, 337 (1971).
  - [22] P. Maier-Komor, P. Glässel, E. Huenges, H. Rösler, H. J. Scheerer, H. K. Vonach, and H. Baier, Z. Phys. **A278**, 327 (1976).
  - [23] S. Landsberger, R. Lecomte, P. Paradis, and S. Monaro, Phys. Rev. C **21**, 588 (1980).
  - [24] J. H. Hirata, Doctoral thesis, Instituto de Física da USP, São Paulo, Brasil, 1984.
  - [25] B. E. Chi, Nucl. Phys. **83**, 97 (1966).

- [26] B. Elbek and P. O. Tjom, *Adv. Nucl. Phys.* **3**, 259 (1969).
- [27] F. S. Stephens, *Rev. Mod. Phys.* **47**, 43 (1975).
- [28] J. Rekstad, *Nucl. Phys.* **A247**, 7 (1975).
- [29] S. Sirota, J. L. M. Duarte, L. B. Horodynski-Matsushigue, and T. Borello-Lewin, *Phys. Rev. C* **40**, 1527 (1989).
- [30] J. M. Arias, C. E. Alonso, and M. Lozano, *Nucl. Phys.* **A466**, 295 (1987).
- [31] G. Maino, A. Ventura, A. M. Bizzeti-Sona, and P. Blasi, *Z. Phys. A* **340**, 241 (1991).